Seasonal rainfall variability in Korea within the context of different evolution patterns of the central Pacific El Niño

Jong-Suk Kim, Chan-Young Son, Young-Il Moon and Joo-Heon Lee

ABSTRACT

This study aims to identify how different evolution patterns of the central Pacific (CP) El Niño influence seasonal rainfall and intense rainfall occurrence in Korea. The results suggest that changes in the CP El Niño can influence the spatiotemporal patterns of seasonal and heavy rainfall over East Asia. Specifically, for the Korean Peninsula, rainfall was typically lower during the years with the abrupt-decaying and prolonged-decaying CP El Niño evolution patterns. During the symmetric-decaying years, more rainfall occurred over the Korean Peninsula, and heavy rainfall events were concentrated in the central regions. Hence, flooding poses a risk to the Korean Peninsula and such risks may be heightened during symmetric-decaying CP El Niño years. Although this study relies on relatively short-term observation events and samples, the results provide a starting point for a more detailed examination of the large-scale and local factors for developing adaptive strategies to protect water resources and to plan for extreme weather events in a changing climate.

Key words | CP El Niño, extreme rainfall, Korean Peninsula, seasonal rainfall, sea surface temperature (SST) evolution

Jong-Suk Kim
State Key Laboratory of Water Resources and Hydropower Engineering Science,
Wuhan University,
Wuhan 430072
China

Chan-Young Son
Young-Il Moon (corresponding author)
Department of Civil Engineering,
University of Seoul,
Seoul, 02504,
South Korea
E-mail: *ymoon@uos.ac.kr*

Young-Il Moon
Urban Flood Research Institute,
University of Seoul,
Seoul, 02504,
South Korea

Joo-Heon Lee
Department of Civil Engineering,
Joongbu University,
KyungGi, 10279,
South Korea

INTRODUCTION

Due to the effects of a changing climate, the frequency and intensity of extreme weather events such as snow, drought, typhoons, heavy rain, and intense heat or cold are changing globally. Studies in this regard are actively being conducted by many researchers worldwide (Kim *et al.* 2006; IPCC 2007; Lau *et al.* 2008; Lau & Zhou 2012; Chang *et al.* 2013). One of the most salient issues regarding climate change is that changes in extreme rainfall events exhibit different regional trends; therefore, communities should prepare for the types of natural disasters that are likely to occur locally (Kim & Jain 2011). In addition, it is crucial that societies establish practical adaptive strategies for dealing with climatic change, such as improving ecological stability and resilience and securing stable water supplies and resources for the coupled human–environmental system (Horel & Wallace 1981; Pizarro & Lall 2002; Wang *et al.* 2008; Wu *et al.* 2009, 2012; Kim & Jain 2011; Kim *et al.* 2012a; Ye 2013).

The occurrences of extreme climatic events and changes in the El Niño pattern are closely associated with each other; specifically, when El Niño occurs, tropical Pacific surface temperature fluctuations are correlated with climatic variability in Pacific Rim countries through air–sea interactions and tropical Pacific mid-latitude teleconnections (Nitta 1987; Wang *et al.* 2000; Kumar *et al.* 2006; Wang & Hendon 2007; Zhao *et al.* 2010; Zheng *et al.* 2012). El Niño patterns are commonly divided into two groups according to the locations where the peak and persistent anomalies in tropical sea surface temperature (SST) occur: (1) the Eastern Pacific (EP) El Niño, which occurs in the EP and (2) the Central Pacific (CP) El Niño, which emerges in the CP (Yeh *et al.* 2009; Yu & Kim 2011; Dewitte *et al.* 2012; Li *et al.* 2013; Yoon *et al.* 2013).

Since the 2000s, there have been more CP El Niño patterns in which the center of the SST warming moves from

doi: 10.2166/wcc.2016.020

the tropical EP to the CP (Kao & Yu 2009; Yeh *et al.* 2009; Lee & McPhaden 2010; Yu *et al.* 2010). This change distinctly influences the movement of air in the Walker circulation contributing to the creation of anomalous cyclones of large-scale circulation patterns located over the east of the Philippines in response to the SST warming in the equatorial CP (Kim *et al.* 2012a, 2012b). During such SST warming events, differences in the process of heat or vapor transport to mid-latitudinal areas from the tropical sea cause regional changes in seasonal rainfall in countries adjacent to the Pacific (Weng *et al.* 2007; Feng *et al.* 2011; Kim *et al.* 2012b; Yoon *et al.* 2013).

Although the dynamic processes of the development and extinction of the CP El Niño are not known in detail, it has been reported that air–sea interactions or the forcing of the large-scale movement of air in the CP region play crucial roles in generating the CP pattern (Ashok *et al.* 2007; Kao & Yu 2009; Yu *et al.* 2010). In addition, analyses of high-resolution climate change scenarios indicate that the strength or frequency of the CP El Niño could increase; thus, the impacts and risks of the CP pattern seem to be of considerable importance (Yeh *et al.* 2009; Lee & McPhaden 2010; Na *et al.* 2011). In East Asia, however, little attention has been given to quantitative studies that investigate the hydrometeorological variables within the context of spatio-temporal patterns of evolving anomalous SST patterns over the CP.

Therefore, the purpose of this study is to classify the different types of the CP El Niño based on changes in SSTs, and to identify the regional changes in intense and heavy rainfall events and seasonal rainfall that are likely to occur in East Asia and over the Korean Peninsula (KP) caused by changing the CP El Niño patterns and associated changes in SSTs. The results of this study may provide foundational information for developing adaptive strategies to protect water resources in changing climatic conditions.

DATA AND METHODS

To extract the CP El Niño information indicative of abnormal increases in SSTs in the CP region, we utilized monthly Niño 3 (5 °S–5 °N, 150 °E–90 °W) and Niño 4 (5 °S–5 °N, 160 °E–150 °W) data and the ERSST_v3 data provided by the National Oceanic and Atmospheric Administration (NOAA 2014). This study employed four methods to classify the CP El Niño. The first method, known as the Niño method, involves the application of Niño 4 > Niño 3 conditions for this period of El Niño development (December–February), as described by Yeh *et al.* (2009). As an addition to this method, Kim *et al.* (2009) defined the CP El Niño as that in which the August–October (ASO) average Niño 3 and Niño 4 indices satisfy two conditions (Niño 3 < 1σ, Niño 4 > 1σ).

The second method is the empirical orthogonal function-based index. This index was first proposed by Kao & Yu (2009), who classified patterns with SST empirical orthogonal functions higher than 1σ and durations of 3 months as a CP El Niño. The El Niño Modoki index (EMI) (Ashok *et al.* 2007), as applied by Yoon *et al.* (2013), is the third method. In this method, the CP El Niño is defined as having a 3-month moving average EMI higher than 0.66 and duration of 6 months from September to February of the following year. Finally, we used the mean CP index (Kao & Yu 2009) to classify CP El Niño as years when the CP index was higher than 1σ. Table 1 provides more detailed information on the CP El Niño events selected in this study. CP El Niño events can be classified into three different groups (prolonged-decaying pattern, abrupt-decaying pattern, and symmetric-decaying pattern)

Table 1 | El Niño classification identified by different definitions

Year	Type of El Niño	Classification methods
1977/1978	CP	A, B, C, D
1987/1988	CP	A, B, D
1990/1991	CP	A, C, D
1991/1992	MIX*(CP/EP) or CP	A*, B, C, D
1994/1995	CP	A, B, C, D
2002/2003	MIX*(CP/EP) or CP	A*, B, C, D
2004/2005	CP	A, B, C, D
2009/2010	CP	A, B, D

CP, Central Pacific El Niño; EP, Eastern Pacific El Niño.
El Niño-type classification: A: NINO method (Yeh *et al.* 2009: Nino 4 > Nino 3 (DJF); Kim *et al.* 2009: Nino 3 < 1σ, Nino 4 > 1σ (ASO)). B: empirical orthogonal function (EOF)-based index (Kao & Yu 2009: SST EOF > 1σ for more than 3 consecutive months). C: EMI method (Yoon *et al.* 2013: EMI (3-month moving average) >0.66 and for more than 6 consecutive months (SONDJF)). D: N_{WP} index (Ren & Jin 2011: $N_{wp} > 1\sigma$ and for more than 3 consecutive months (DJF)).

according to the evolution patterns of the SSTs in the central region of the Pacific Ocean (Yu & Kim 2010).

First, in the prolonged-decaying pattern (Figure 1(a)), the warm SST is generated in the equatorial Pacific region and reaches its peak between December and February. The decline of the SST is relatively slow compared to the other two patterns. Second, in the case of the abrupt-decaying pattern (Figure 1(b)), abnormal SST rapidly declines as the force that develops in the eastern region of the Pacific Ocean encounters the strong negative SST anomalies. Finally, in the case of the symmetric-decaying pattern (Figure 1(c)), an increase in the SST occurs in the CP between October and January and the decline of the SST is slower than that of the abrupt-decaying pattern, with the advancement and decline of the SST being symmetrical in general. The three CP El Niño patterns might significantly influence the global weather and climate system.

In this study, monthly rainfall data obtained from the Global Precipitation Climatology Center, which combines station-based records and grid-based global precipitation using satellite imagery, with $0.5^\circ \times 0.5^\circ$ resolution, were used to analyze the characteristics of seasonal rainfall in East Asia (20 °N–60 °N, 100 °E–150 °E) between 1979 and 2010. In addition, this study used daily rainfall data for the period 1973–2010, obtained from 57 observatories managed by the Korea Meteorological Administration (KMA) to analyze the characteristics of rainfall in the KP (Figure 2 and Table 2). For the composite analysis, data were sorted into

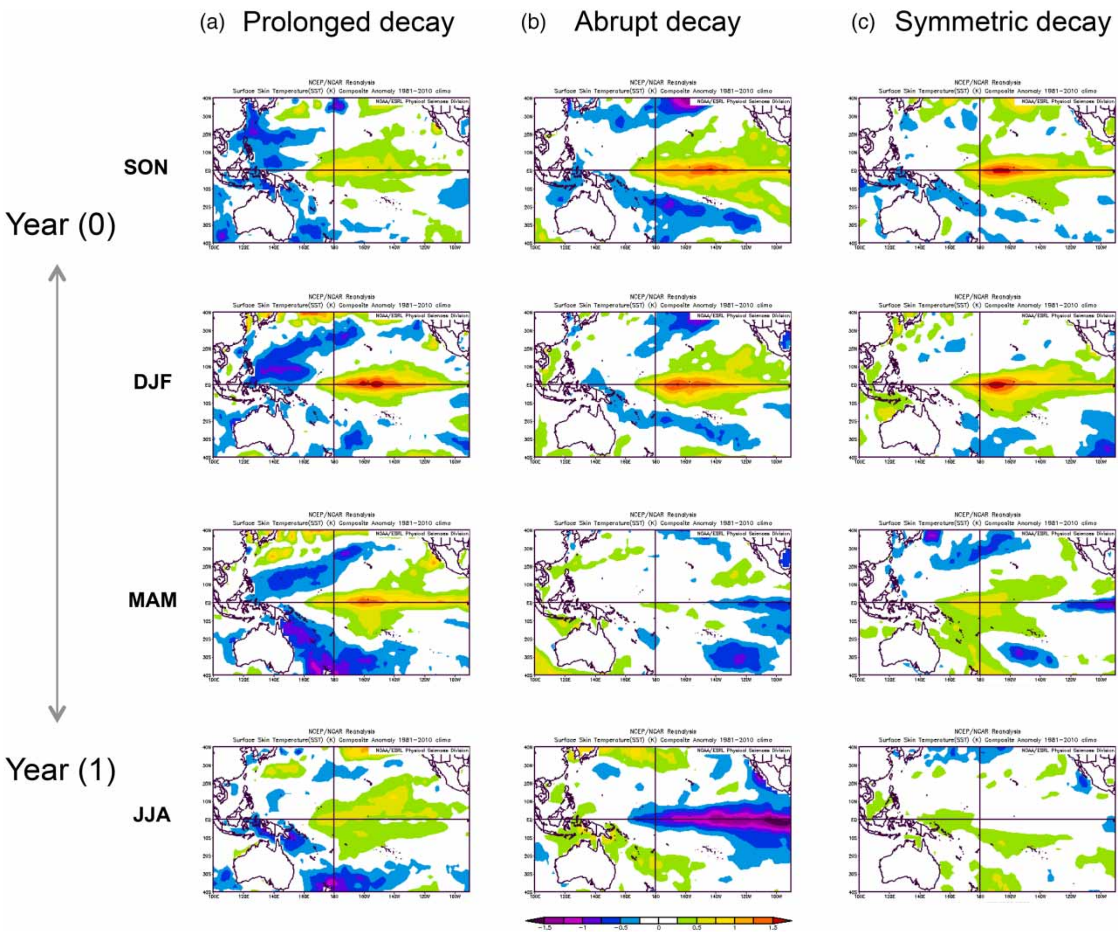

Figure 1 | Composite anomalies of SST according to different evolution patterns of the CP El Niño during September–November (SON) of the El Niño developing year (0) to June–August of the following year (1): (a) prolonged-decaying years (1990/1991, 1991/1992); (b) abrupt-decaying years (1977/1978, 1987/1988, 2009/2010); and (c) symmetric-decaying years (1994/1995, 2002/2003, 2004/2005).

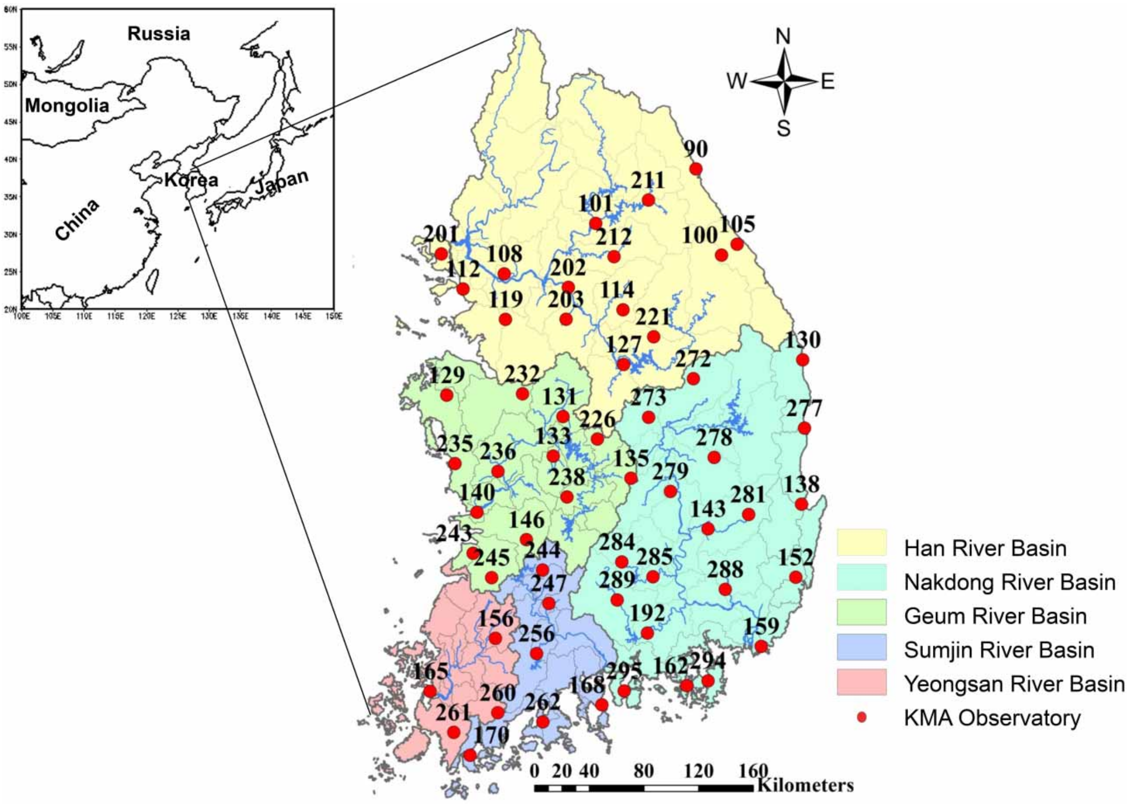

Figure 2 | The five major river basins in Korea and the KMA observatory locations.

Table 2 | Rainfall information of Korea's five major river basins (1973–2010)

Basins	Area (km^2)	Annual rainfall (mm)	Spring rainfall (mm)	Summer rainfall (mm)	Daily peak rainfall (mm)
Han River	38,421.8	1,237.2	201.9	748.9	163.4
Nakdong River	31,712.0	1,165.4	229.7	648.0	164.8
Geum River	17,537.0	1,229.1	217.7	701.5	159.8
Seomjin River	8,299.1	1,384.9	258.9	780.4	197.0
Yeongsan River	7,598.7	1,303.1	246.7	709.0	262.3

categories and comparing means for different CP El Niño categories. A composite analysis was applied for the climatology of the period 1981–2010 to examine the changing patterns of seasonal rainfall and extreme rainfall in East Asia including the KP. To complement the relatively low number of CP El Niño events, the bootstrap random resampling technique, which is commonly used in statistical analysis and applied hydroclimatological studies (Ripley 1987; Becker *et al.* 1988; Kundzewicz & Robson 2000), was employed by using 1,000 subsets of different CP El Niños with random replacement from historical observations (1973–2010), and the statistical test was performed at 90% confidence level.

ANALYSIS AND RESULTS

Seasonal rainfall during the CP El Niño

During the prolonged-decaying years, spring rainfall was high in many East Asia regions (Figure 3(a)), compared to normal years (1981–2010). Increases in spring rainfall were observed

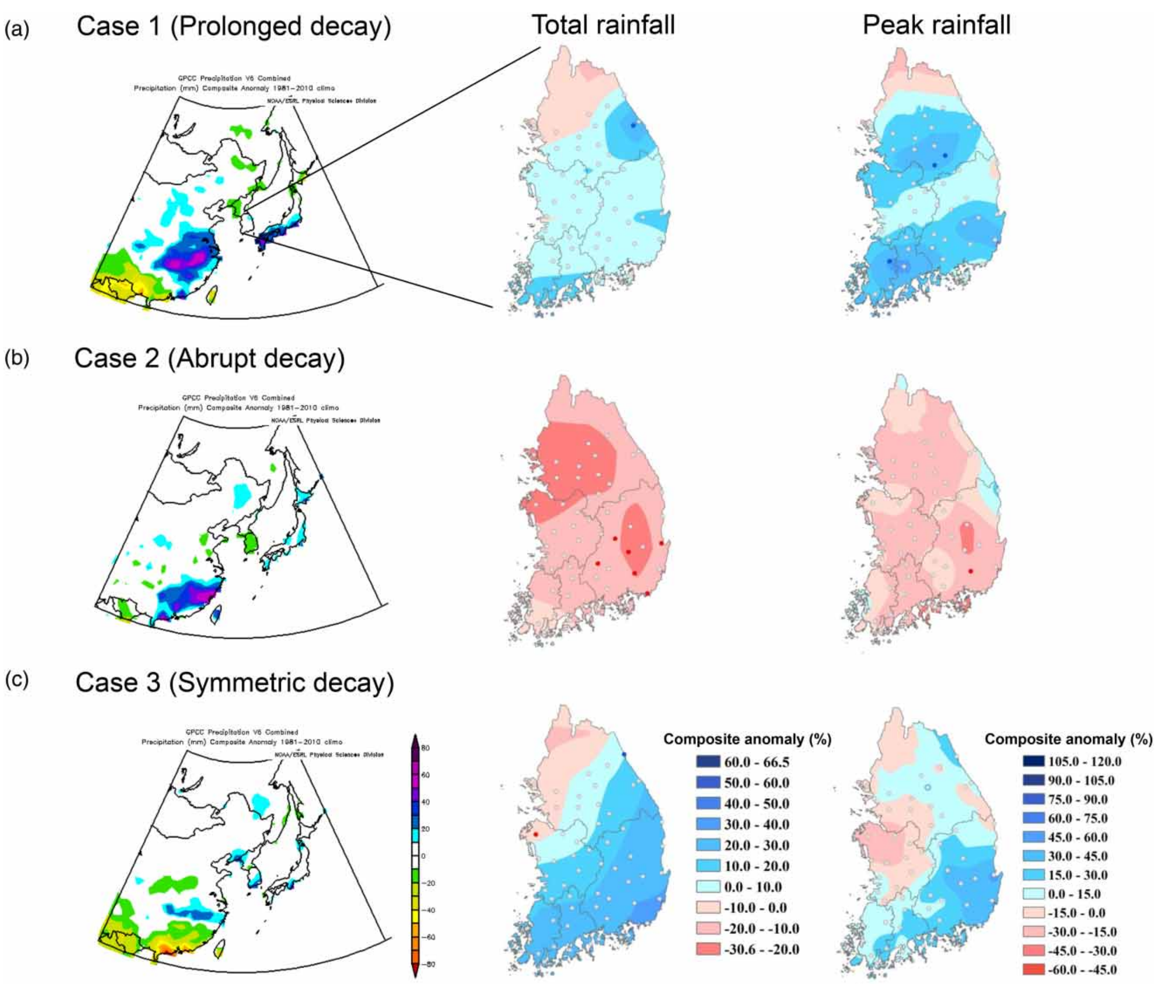

Figure 3 | Percentage changes in the composite anomalies of spring rainfall and daily peak rainfall (March–May) according to three evolution patterns of the CP El Niño: (a) Case 1 (prolonged decay); (b) Case 2 (abrupt decay); and (c) Case 3 (symmetric decay). For each case, circle symbols show statistically significant positive (negative) anomalies of spring rainfall with a 90% confidence limit.

for several locations in the eastern region of China (the Yangtze River, the Huaihua basin, and southeast coastal areas), whereas spring rainfall in the southwestern region of China (Taiwan and the Pearl River basin) decreased. In Japan, increases in spring rainfall were observed in the southern and central regions (Kyushu, Shikoku, Chukoku, Kansai, Tokai, and Kanto). On the Korean Peninsula, except for the northern region, an overall increasing pattern in spring rainfall was observed, but the effect was relatively insignificant. These changes in rainfall patterns are similar to the springtime daily peak; relatively high rainfall events were found in the central and southern part of Korea.

During the abrupt-decaying years, increases in spring rainfall were observed in many southeastern regions of China (the Pearl River basin, southeast coastal areas, and the southern basin of the Yangtze River), compared to normal years (Figure 3(b)). In Japan, some regions showed increases in spring rainfall, but the overall influence was insignificant. In contrast, the KP experienced decreases in spring rainfall (up to −31.6%), compared to normal years for all regions. In particular, six observation points within the Nakdong River basin observed statistically significant decreases in rainfall. For the spring peak rainfall events, no statistically significant changes were found.

During the symmetric-decaying years (Figure 3(c)), increases in spring rainfall were observed in the Yangtze River and some parts of southeastern China near coastal areas, but relatively strong decreases in spring rainfall were observed in the other southern regions (Taiwan, the Pearl River basin, and the upper region of the Yangtze River). In contrast, increases in spring rainfall were observed in all parts of the KP, except for the Han River and some parts of the Geum River basin. Increases in spring rainfall were most pronounced in the southern region of the KP. The occurrence of the peak was relatively higher in the Nakdong River basin.

Summer rainfall during the prolonged-decaying years decreased in many parts of the East Asian region (Figure 4). Decreases in summer rainfall were observed in the southwestern regions of China, with the exception of the mouth of the Yangtze River (Jiangsu, Shanghai, and Anhui) near the East China Sea; however, the northern regions of China (the Heirongjiang River and the Liao-ho River basin) experienced increases in summer rainfall. In Japan, the southern region (Kyushu and Shikoku) and northern region (Tohoku) experienced increases in summer rainfall compared to normal years. In some parts of the southeastern regions of the KP, similar to China, increases in summer rainfall were observed. However, most regions in Korea experienced decreases in rainfall (up to −39.0%). The seven observation points in the Han River region recorded particularly pronounced and statistically significant patterns of decreases in summer rainfall.

During the abrupt-decaying years, the middle and eastern regions of Asia experienced increases in summer rainfall, but the southern regions of China experienced

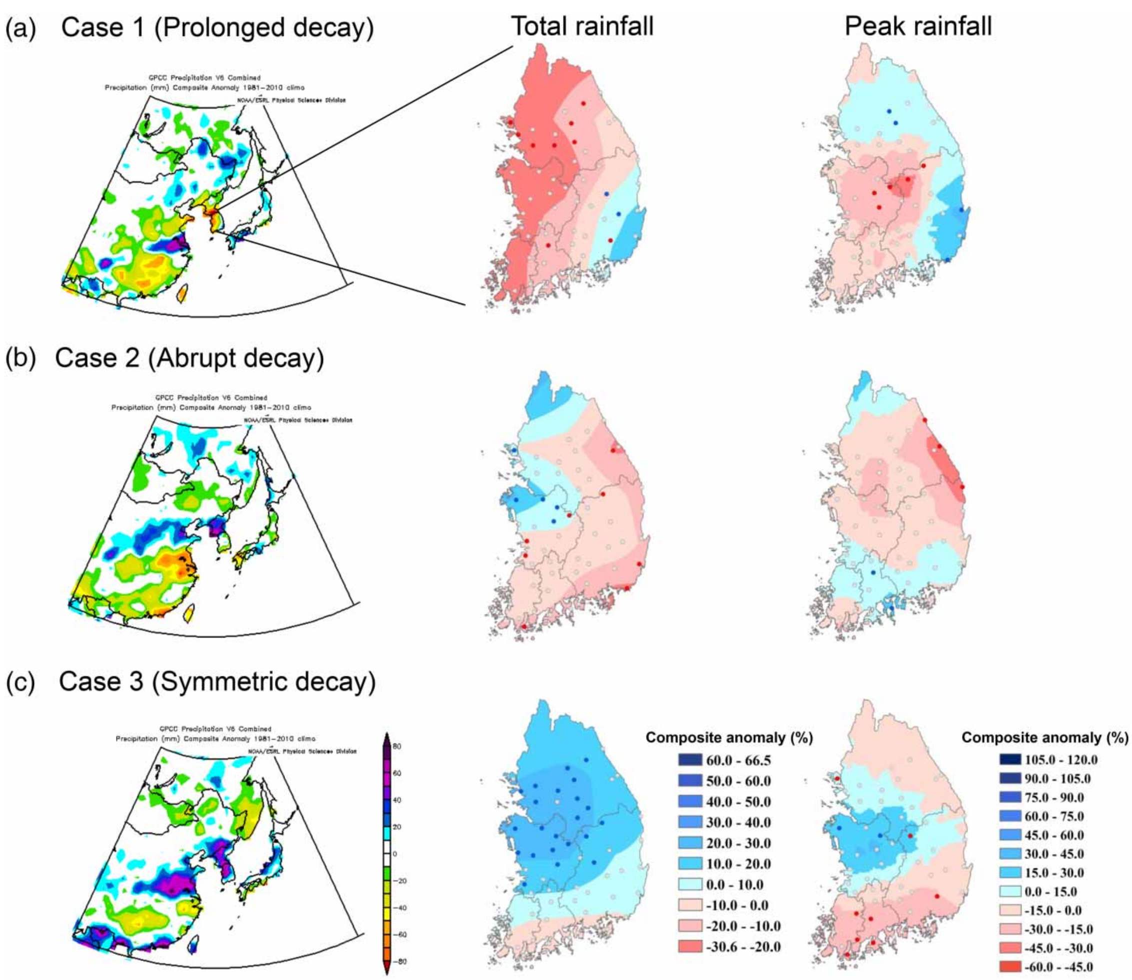

Figure 4 | Percentage changes in the composite anomalies of summer rainfall and daily peak rainfall (June–August) according to three evolution patterns of the CP El Niño: (a) Case 1 (prolonged decay); (b) Case 2 (abrupt decay); and (c) Case 3 (symmetric decay). For each case, circle symbols show statistically significant positive (negative) anomalies of summer rainfall with a 90% confidence limit.

overall decreases compared to normal years. In particular, in the Yangtze River, the Haiha basin, and the southeastern coastal areas, relatively large decreases in summer rainfall were observed. In Japan, most regions experienced decreases in summer rainfall except for some central regions. Like the middle and eastern regions in China, the northern regions of the KP experienced increases in summer rainfall, whereas the eastern and southern regions experienced decreases compared to normal years.

Finally, during the symmetric-decaying years, increases in summer rainfall compared to normal years were observed in the eastern (the Haiha basin and the Yellow River basin) and southern regions (Taiwan and the Pearl River basin) of China. Likewise, increases in summer rainfall were observed in the northern regions of Japan. However, the eastern regions of China (the Yangtze River basin and some parts of the southeast near coastal waters) generally experienced significant decreasing patterns in summer rainfall. In all basins in the KP, including those in North Korea, increases in summer rainfall were observed (up to 40.3%), based on a 20-year climatology (1981–2010). A total of 22 observation points (10 points in the Han River basin, nine points in the Geum River basin, and three points in the Nakdong River basin) recorded statistically significant increases. This indicates that Korea may face a higher risk of flooding during the symmetric-decaying CP El Niño evolution pattern. For the summer peak rainfall, significant changes were not detected, but in the case of daily peak rainfall, the patterns of contrasting wet and dry episodes between the central and southern regions of the KP were found during symmetric-decaying years.

Extreme rainfall variability during the CP El Niño

Figure 5 shows the spatiotemporal changes in peak rainfall over the KP during the three CP El Niño evolution patterns at the onset of annual peak rainfall (Figure 5(a)). During the prolonged-decaying and symmetric-decaying years, the onset of annual peak rainfall was slightly delayed. In contrast, the annual peak rainfall occurrence for the abrupt-decaying years was relatively early compared to normal years. During the prolonged-decaying years, increases in peak rainfall (up to 73.7%) were observed in the central

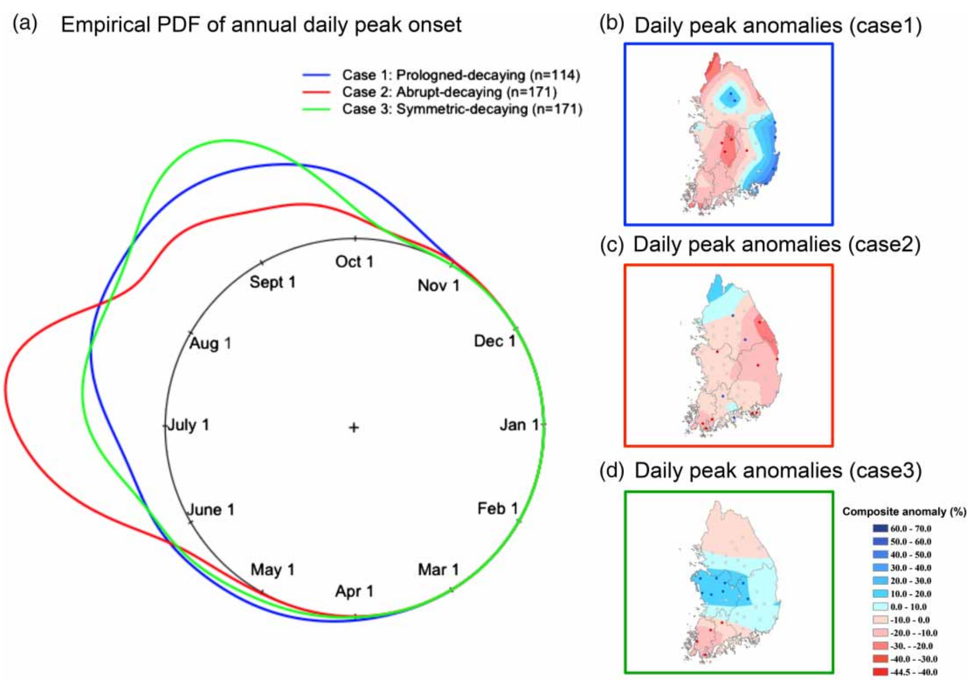

Figure 5 | Composite anomalies of daily peak rainfall events for the three evolution patterns of the CP El Niño: (a) empirical PDF of annual daily peak onset; (b) annual peak in daily rainfall (prolonged decay); (c) annual peak in daily rainfall (abrupt decay); and (d) annual peak in daily rainfall (symmetric decay). For each case (b)–(d), circle symbols show statistically significant positive (negative) anomalies of summer rainfall with a 90% confidence limit.

regions of the Han River basin and the eastern regions of the Nakdong River basin, but the Geum River, Seomjin River, and Yeongsan River basins experienced decreases (up to −52.3%) in peak rainfall compared to normal years (Figure 5(b)). During the abrupt-decaying years, decreases (up to −48.2%) in peak rainfall were observed in most areas except for the northern regions of the Han River basin. Nine observation points recorded a pronounced and statistically significant decreasing pattern (Figure 5(c)). During the symmetric-decaying years, statistically significant increases (up to 54.23%) in annual peak rainfall were observed in the central regions of the KP, including the southern parts of the Han River, Geum River, and Nakdong River basins. Conversely, the northern part of the Han River, Seomjin River, and Yeongsan River basins experienced decreases in annual peak rainfall (up to −47.0%) compared to normal years (Figure 5(d)).

To understand the characteristics of local changes in extreme hydrological events associated with evolution of each CP El Niño pattern, analyses of the frequencies of rainfall events were also conducted (Figure 6). For the total annual number of days of rainfall, no large differences were found for the prolonged-decaying (with an average of 108.4 days and a coefficient of variation (CV) of 0.128), abrupt-decaying (with an average of 106.4 days and a CV of 0.168), or symmetric-decaying (with an average of 105.5 days and a CV of 0.168) years, compared to normal years. However, analyses of the number of days of heavy rain (defined as ≥80 mm/day, which used the threshold of the heavy rain advisory in Korea) revealed differences according to the CP El Niño evolution patterns. Specifically, there were fewer heavy rain days during the prolonged-decaying (with an average of −2.2 days and a CV of 0.762) and abrupt-decaying (with an average of −1.9 days and a CV of 0.803) years, while there were more heavy rain days during the symmetric-decaying years (with an average of 2.7 days and a CV of 0.735). The range of fluctuation for the symmetric-decaying of CP El Niño was relatively smaller than that of the other two CP El Niño patterns. In particular, for the Han River basin, the number of rainfall days above 80 mm/day increased by up to 2.77 days, compared to normal years, and 17 observation points recorded statistically significant increasing patterns.

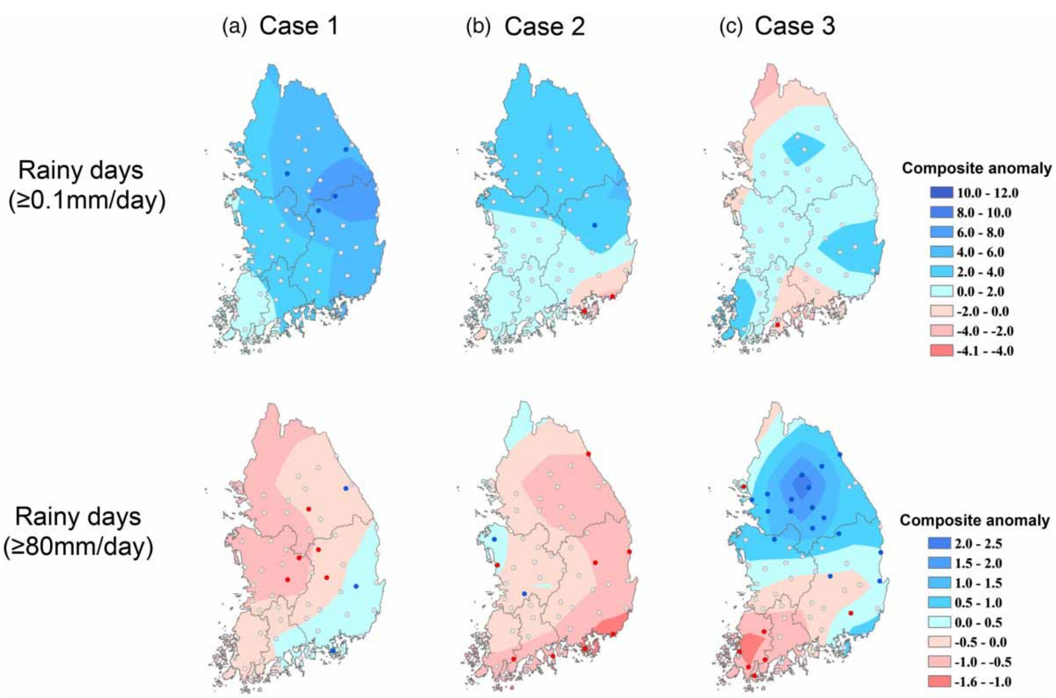

Figure 6 | Composite anomalies of rainy days (≥0.1 mm/day and ≥80 mm/day) for the three evolution patterns of the CP El Niño: (a) Case 1 (prolonged decay); (b) Case 2 (abrupt decay); and (c) Case 3 (symmetric decay). For each case, circle symbols show statistically significant positive (negative) anomalies of summer rainfall with a 90% confidence limit.

SUMMARY AND CONCLUSIONS

This study analyzed changes in seasonal rainfall for the East Asian region during various evolving and declining patterns of the CP El Niño. In addition, spatiotemporal patterns of change for extreme hydrological events were analyzed for the KP. The following conclusions were derived from the results:

1. For the prolonged-decaying years during a CP El Niño, seasonal spring rainfall showed strong increases in the eastern regions of China and the southern regions of Japan. For the entire KP, except for the northern region of Han River, increases in spring rainfall compared to normal years were detected, but the change was generally small. Less summer rainfall occurred during the prolonged-decaying years in most regions except for the mouth of the Yangtze River, the southern part of Japan, and the southeastern parts of the KP.
2. For the abrupt-decaying years during a CP El Niño, increases in spring rainfall were detected across portions of China and some parts of the KP, but decreases in spring rainfall were also apparent. Much of the summer rainfall during abrupt-decaying years occurred in the shape of a band in the middle and eastern regions of China and in the northern regions of the KP. However, the southeastern regions of the KP, the southern regions of China, and several regions of Japan experienced less rainfall during this type of CP El Niño pattern.
3. For the symmetric-decaying years during a CP El Niño, spring rainfall showed clear decreasing patterns in the southern region of China. However, significantly increasing patterns were detected in coastal areas in China, the Yangtze River basin, and in the southern regions of the KP. For summer rainfall, the eastern regions of China and the southern regions of Japan experienced only small amounts of rainfall, but the eastern and southern regions of China, the northern regions of Japan, and the entire landmass of the KP experienced more rainfall than normal years.
4. The results from analyses of the frequency of annual daily peak rainfall events indicated that for the prolonged-decaying years and abrupt-decaying years, the number of extreme storm occurrences ($\geq$80 mm/day) was lower than that of normal years for many parts of the KP, excluding some basins of the Nakdong River. However, there were more heavy rain days during the symmetric-decaying years than during the normal years. The Han River basin, including the central regions, exhibited a significant increasing pattern.
5. Finally, annual daily peak rainfall increased in the Han River area and the eastern coast of Nakdong River during the prolonged-decaying years. In the western and southern regions of the KP, annual daily peak rainfall decreased somewhat, compared to normal years. For the abrupt-decaying years, the number of days with annual daily peak rainfall was generally lower than that of normal years; this was especially pronounced in the eastern region of the KP. For the symmetric-decaying years, the central regions of the KP experienced a statistically significant increase in the number of days with peak rainfall, whereas the northern and southern regions of the KP experienced fewer days of annual daily peak rainfall. The incidence period of the peak rainfall during the prolonged-decaying and symmetric-decaying years occurred later in the year, whereas rainfall during the abrupt-decaying years started earlier in the year than that of normal years.

In summary, although this study relies on relatively short observation events and samples, the results suggest that changes in the CP El Niño pattern can influence spatiotemporal patterns of seasonal and heavy rainfall over East Asia. We hope that the findings from this study will be useful in analyzing and securing water resources under different climate change scenarios and in establishing medium- and long-term flood control strategies. Given the strong seasonality and importance of water supplies in the East Asian region, further investigation of air–sea interactions based on robust numerical simulations will be required to obtain reliable results on regional hydrometeorological variability and different evolution patterns of the CP El Niño.

ACKNOWLEDGEMENTS

This work was supported by the 2016 Research Fund of the University of Seoul. This research was also supported by a grant (17AWMP-B079625-04) from the Water Management Research Program funded by the Ministry of Land, Infrastructure and Transport of the Korean Government.

REFERENCES

Ashok, K., Behera, S. K., Rao, S. A., Weng, H. & Yamagata, T. 2007 El Niño Modoki and its teleconnection. *J. Geophys. Res.* **112**, C11007. doi:10.1029/2006 JC003798.

Becker, R. A., Chambers, J. M. & Wilks, A. R. 1988 *The New S Language: A Programming Environment for Data Analysis and Graphics*. Wadsworth & Brooks/Cole Advanced Books & Software, Monterey, CA, USA.

Chang, C. P., Yang, Y. T. & Kuo, H. C. 2013 Large increasing trend of tropical cyclone rainfall in Taiwan and the roles of terrain. *J. Climate* **26**, 4138–4147.

Dewitte, B., Choi, J., An, S. I. & Thual, S. 2012 Vertical structure variability and equatorial waves during central Pacific and eastern Pacific El Niño in a coupled general circulation model. *Clim. Dyn.* **38**, 2275–2289.

Feng, J., Chen, W., Tam, C. Y. & Zhou, W. 2011 Different impacts of El Niño and El Niño Modoki on China rainfall in the decaying phases. *Int. J. Climatol.* **32**, 2091–2101.

Horel, J. D. & Wallace, J. M. 1981 Planetary-scale atmospheric phenomena associated with the Southern Oscillation. *Mon. Weather Rev.* **109**, 813–829.

IPCC 2007 *The physical science basis. Contribution of Working Group I to the Fourth Assessment Report of the Intergovernmental Panel on Climate Change*. Cambridge University Press, Cambridge.

Kao, H. Y. & Yu, J. Y. 2009 Contrasting eastern-Pacific and central-Pacific types of El Niño. *J. Climate* **22**, 615–632. doi:10.1175/2008JCLI2309.1.

Kim, J. S. & Jain, S. 2011 Precipitation trends over the Korean peninsula: typhoon-induced changes and a typology to characterize climate related risk. *Environ. Res. Lett.* **6**, 034033.

Kim, J. H., Ho, C. H., Lee, M. H., Jeong, J. H. & Chen, D. 2006 Large increase in heavy rainfall associated with tropical cyclone landfalls in Korea after the late 1970s. *Geophys. Res. Lett.* **33**, L18706. doi:10.1029/2006GL027430.

Kim, H., Webster, P. J. & Curry, J. A. 2009 Impact of shifting patterns of Pacific Ocean warming on north Atlantic tropical cyclones. *Science* **325**, 77–80. doi:10.1126/science.1174062.

Kim, J. S., Li, R. C. Y. & Zhou, W. 2012a Effects of the Pacific-Japan teleconnection pattern on tropical cyclone activity and extreme events over the Korean peninsula. *J. Geophys. Res.* **117**, D18109.

Kim, J. S., Zhou, W., Wang, X. & Jain, S. 2012b El Niño Modoki and the summer precipitation variability over South Korea: a diagnostic study. *J. Meteorolog. Soc. Jpn* **90** (5), 673–684.

Kumar, K. K., Rajagopalan, B., Hoerling, M., Bates, G. & Cane, M. 2006 Unraveling the mystery of Indian monsoon failure during El Niño. *Science* **314**, 115–119. doi:10.1126/science.1131152

Kundzewicz, Z. W. & Robson, A. J. 2000 *Detecting Trend and Other Changes in Hydrological Data*. Word Climate Program-Data and Monitoring. World Meteorological Organization, Geneva (WMO/TD-No. 1013).

Lau, W. K. M. & Zhou, Y. P. 2012 Observed recent trends in tropical cyclone rainfall over the North Atlantic and the North Pacific. *J. Geophys. Res.* **117**, D03104. doi:10.1029/2011JD016510.

Lau, W. K. M., Zhou, Y. P. & Wu, H. T. 2008 Have tropical cyclones been feeding more extreme rainfall? *J. Geophys. Res.* **113**, D23113. doi:10.1029/2008JD009963.

Lee, T. & McPhaden, M. J. 2010 Increasing intensity of El Niño in the central-equatorial Pacific. *Geophys. Res. Lett.* **37**, L14603. doi:10.1029/2010GL044007.

Li, G., Li, C., Tan, Y. & Pan, J. 2013 Impacts of the central and eastern Pacific types of ENSO on sea surface temperature in the South Pacific. *Theor. Appl. Climatol.* **114**, 315–327. doi:10.1007/s00704-013-0840-1.

Na, H. N., Jang, B. G., Choi, W. M. & Kim, K. Y. 2011 Statistical simulations of the future 50-year statistics of cold-tongue El Niño and warm-pool El Niño. *Asia-Pacific J. Atmos. Sci.* **47** (3), 223–233.

Nitta, T. 1987 Convective activities in the tropical western Pacific and their impact on the Northern Hemisphere summer circulation. *J. Meteorolog. Soc. Jpn* **65**, 373–390.

NOAA (National Weather Service Climate Prediction Center) 2014 Available from: www.cpc.ncep.noaa.gov/data/indices/ (accessed January 2014).

Pizarro, G. & Lall, U. 2002 El Niño-induced flooding in the US West: what can we expect? *EOS Trans. Am. Geophys. Union* **83**, 349–352.

Ren, H. L. & Jin, F. F. 2011 Nino indices for two types of ENSO. *Geophys. Res. Lett.* **38**, L04704. doi:10.1029/2010GL046031.

Ripley, B. D. 1987 *Stochastic Simulation*. John Wiley & Sons Inc., New York, USA.

Wang, G. & Hendon, H. H. 2007 Sensitivity of Australian rainfall to inter-El Niño variations. *J. Climate* **20**, 4211–4226. doi:10.1175/JCLI4228.1.

Wang, Z. M., Ren, X. S. & Guo, H. Y. 2000 *Hai Water Resources Facing the 21st Century*. Tianjin Sciences and Technology Press, Tianjin, China.

Wang, B., Wu, Z., Li, J., Liu, J., Chang, C. P., Ding, Y. & Wu, G. 2008 How to measure the strength of the East Asian Summer Monsoon. *J. Climate* **21**, 4449–4463. doi:10.1175/2008jcli2183.1.

Weng, H., Ashok, K., Behera, S., Rao, S. & Yamagata, T. 2007 Impacts of recent El Niño Modoki on dry/wet conditions in the Pacific Rim during boreal summer. *Clim. Dyn.* **29**, 113–129.

Wu, Z., Wang, B., Li, J. & Jin, F. F. 2009 An empirical seasonal prediction model of the east Asian summer monsoon using ENSO and NAO. *J. Geophys. Res.* **114**, D18120. doi:10.1029/2009jd011733.

Wu, Z., Li, J., Jiang, Z., He, J. & Zhu, X. 2012 Possible effects of the North Atlantic Oscillation on the strengthening relationship between the East Asian Summer monsoon and ENSO. *Int. J. Climatol.* **32**, 794–800. doi:10.1002/joc.2309.

Ye, J. S. 2013 Trend and variability of China's summer precipitation during 1955–2008. *Int. J. Climatol.* **34**, 559–566. doi:10.1002/joc.3705.

Yeh, S. W., Kug, J. S., Dewitee, B., Kwon, M. H., Kirtman, B. P. & Jin, F. F. 2009 El Niño in a changing climate. *Nature* **461**, 511–514. doi:10.1038/nature08316.

Yoon, S. K., Kim, J. S., Lee, J. H. & Moon, Y. I. 2013 Hydrometeorological variability in the Korean Han River Basin and its sub-watersheds during different El Niño phases. *Stoch. Environ. Res. Risk Assess.* **27**, 1465–1477.

Yu, J. Y. & Kim, S. T. 2010 Three evolution patterns of Central-Pacific El Niño. *Geophys. Res. Lett.* **37**, L08706.

Yu, J. Y. & Kim, S. T. 2011 Relationships between extratropical sea level pressure variations and the Central Pacific and Eastern Pacific types of ENSO. *J. Climate* **24**, 708–720.

Yu, J. Y., Kao, H. Y. & Lee, T. 2010 Subtropics-related interannual sea surface temperature variability in the equatorial central Pacific. *J. Climate* **23**, 2869–2884.

Zhao, H. K., Wu, L. G. & Zhou, W. C. 2010 Assessing the influence of the ENSO on tropical cyclone prevailing tracks in the western North Pacific. *Adv. Atmos. Sci.* **27**, 1361–1371. doi:10.1007/s00376-010-9161-9.

Zheng, F., Wan, L. Y. & Wang, H. 2012 Distinguished effects of interannual salinity variability on the development of the Central-Pacific El Niño events. *Atmos. Ocean. Sci. Lett.* **5** (2), 123–127.

First received 5 February 2015; accepted in revised form 5 September 2016. Available online 5 December 2016